

PEARL

**Archaeal and bacterial glycerol dialkyl glycerol tetraether (GDGT) lipids in environmental samples by high temperature-gas chromatography with flame ionisation and time-of-flight mass spectrometry detection**

Lengger, Sabine K.; Sutton, Paul A.; Rowland, Steven J.; Hurley, Sarah J.; Pearson, Ann; Naafs, B. David A.; Dang, Xinyue; Inglis, Gordon N.; Pancost, Richard D.

**Published in:**  
Organic Geochemistry

**DOI:**  
[10.1016/j.orggeochem.2018.03.012](https://doi.org/10.1016/j.orggeochem.2018.03.012)

**Publication date:**  
2018

**Document version:**  
Other version

**Link:**  
[Link to publication in PEARL](#)

**Citation for published version (APA):**

Lengger, S. K., Sutton, P. A., Rowland, S. J., Hurley, S. J., Pearson, A., Naafs, B. D. A., Dang, X., Inglis, G. N., & Pancost, R. D. (2018). Archaeal and bacterial glycerol dialkyl glycerol tetraether (GDGT) lipids in environmental samples by high temperature-gas chromatography with flame ionisation and time-of-flight mass spectrometry detection. *Organic Geochemistry*, 121(0), 10-21. <https://doi.org/10.1016/j.orggeochem.2018.03.012>

## Supplementary to:

### **Archaeal and bacterial glycerol dialkyl glycerol tetraether (GDGT) lipids in environmental samples by high temperature-gas chromatography with flame ionisation and time-of-flight mass spectrometry detection**

*Sabine K. Lengger<sup>a,b,\*</sup>, Paul A. Sutton<sup>b</sup>, Steven J. Rowland<sup>b</sup>, Sarah J. Hurley<sup>c</sup>, Ann Pearson<sup>c</sup>,  
B. David A. Naafs<sup>a</sup>, Xinyue Dang<sup>d</sup>, Gordon N. Inglis<sup>a</sup>, and Richard D. Pancost<sup>a</sup>*

*<sup>a</sup> Organic Geochemistry Unit and The Cabot Institute, School of Chemistry, University of Bristol, Bristol, UK.*

*<sup>b</sup> Petroleum and Environmental Geochemistry Group, Biogeochemistry Research Centre, School of Geography, Earth and Environmental Sciences, University of Plymouth, Plymouth, UK.*

*<sup>c</sup> Department of Earth and Planetary Sciences, Harvard University, Cambridge, MA, USA.*

*<sup>d</sup> State Key Laboratory of Biogeology and Environmental Geology, School of Earth Science, China University of Geosciences, Wuhan, 430074 China.*

*\* corresponding author: School of Geography, Earth and Environmental Sciences, University of Plymouth, Plymouth PL4 8AA, United Kingdom.*

*telephone: +44(0)1752 585 966, email: sabine.lengger@plymouth.ac.uk*

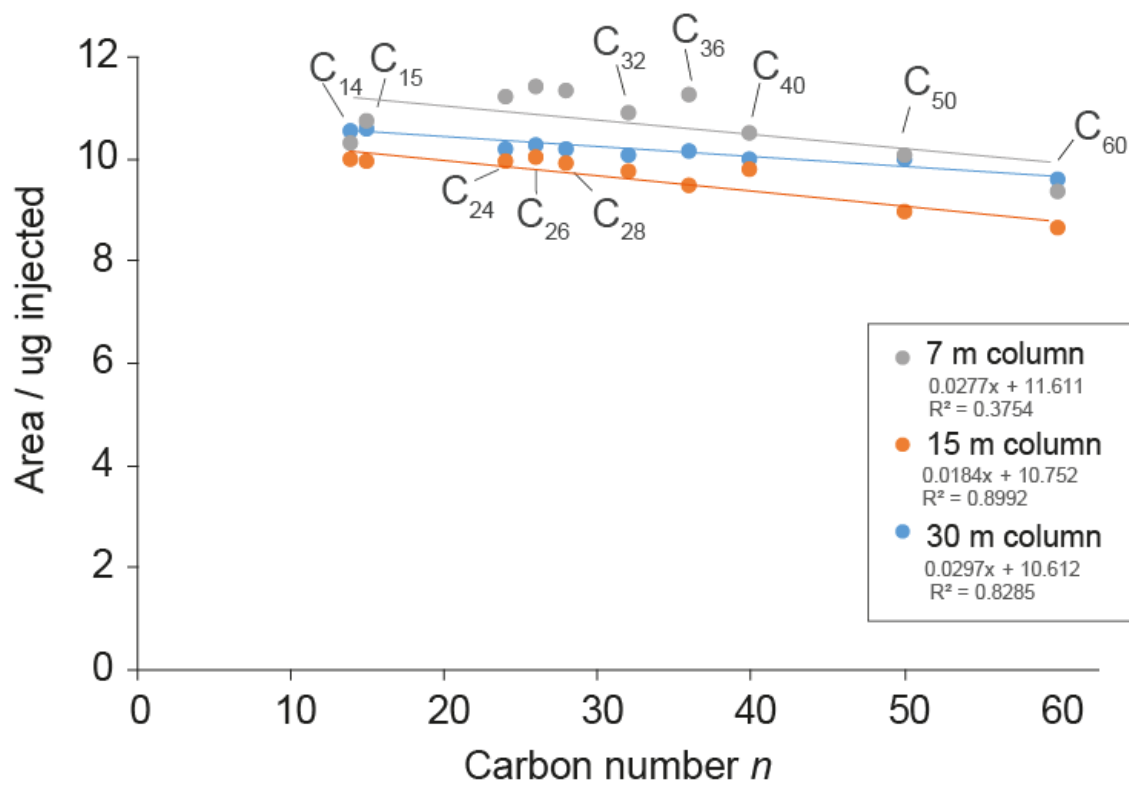


Figure S1. Sensitivities for compounds analysed using HTGC-FID. Areas of *n*-alkanes (14, 15, 24, 26, 28, 32, 36, 40, 50, 60 C) analysed using a 30, 15 and 7 m column normalised on their respective mass (ng) on-column.

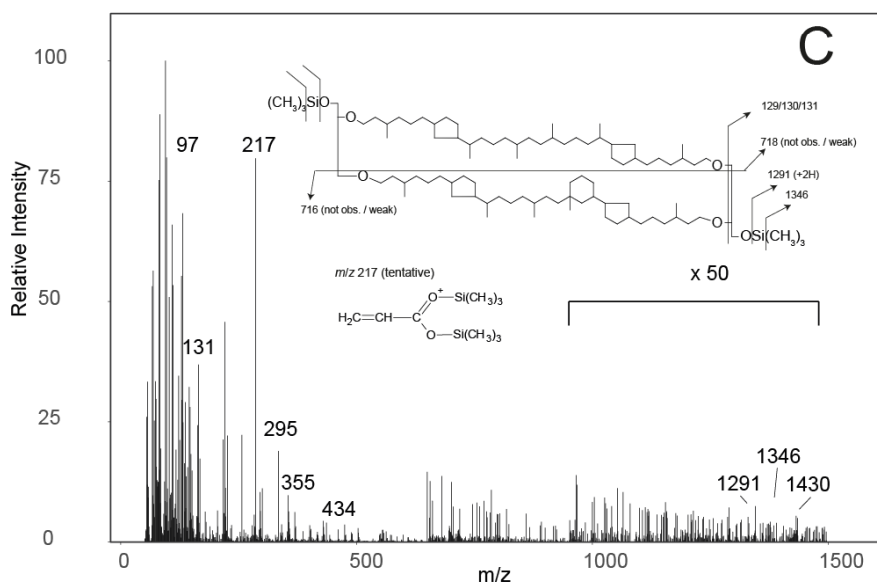
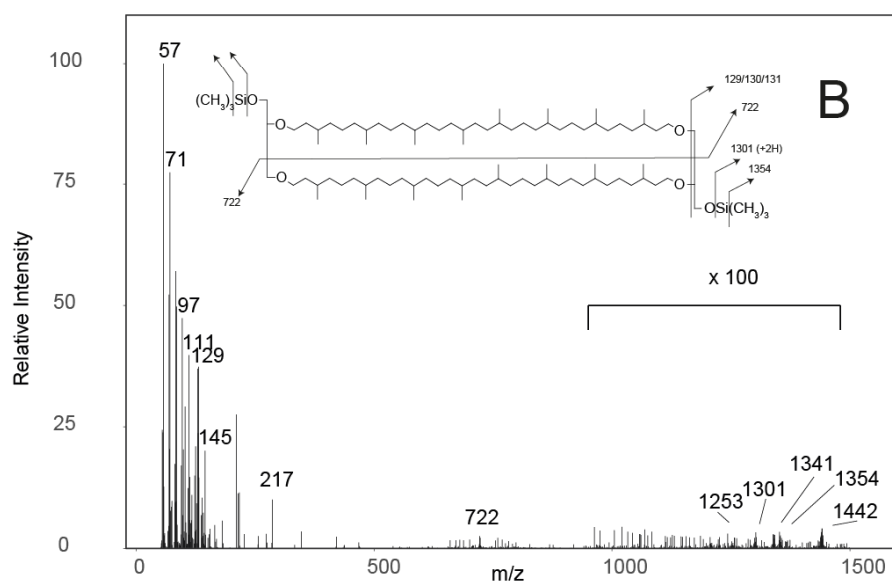
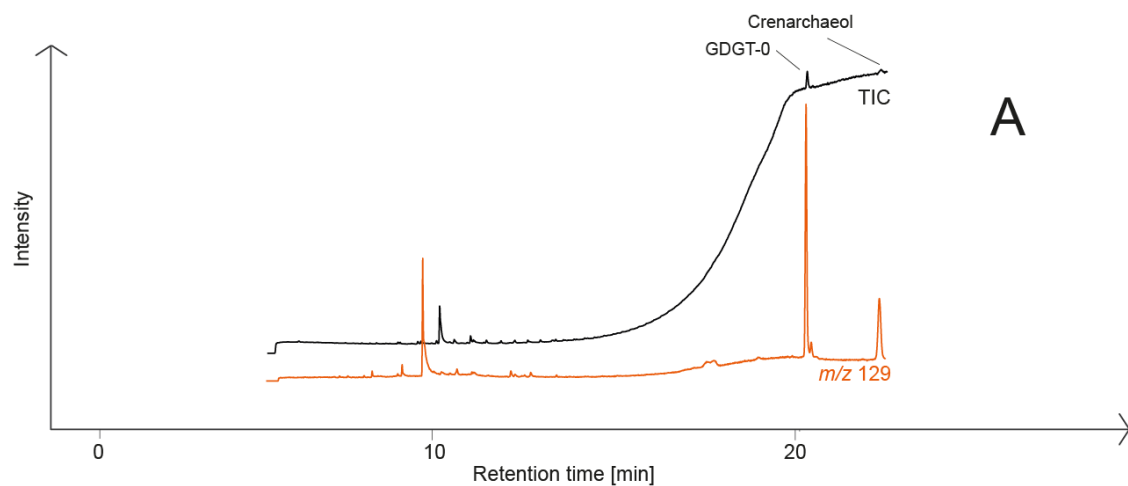


Figure S2. Trimethylsilylated GDGT-0 and crenarchaeol standards analysed using HTGC-TOFMS. A) TIC and extracted ion current of  $m/z$  129, B) 70eV mass spectrum of GDGT-0 and C) 70eV mass spectrum of crenarchaeol. Fragmentation patterns are shown for both molecules.

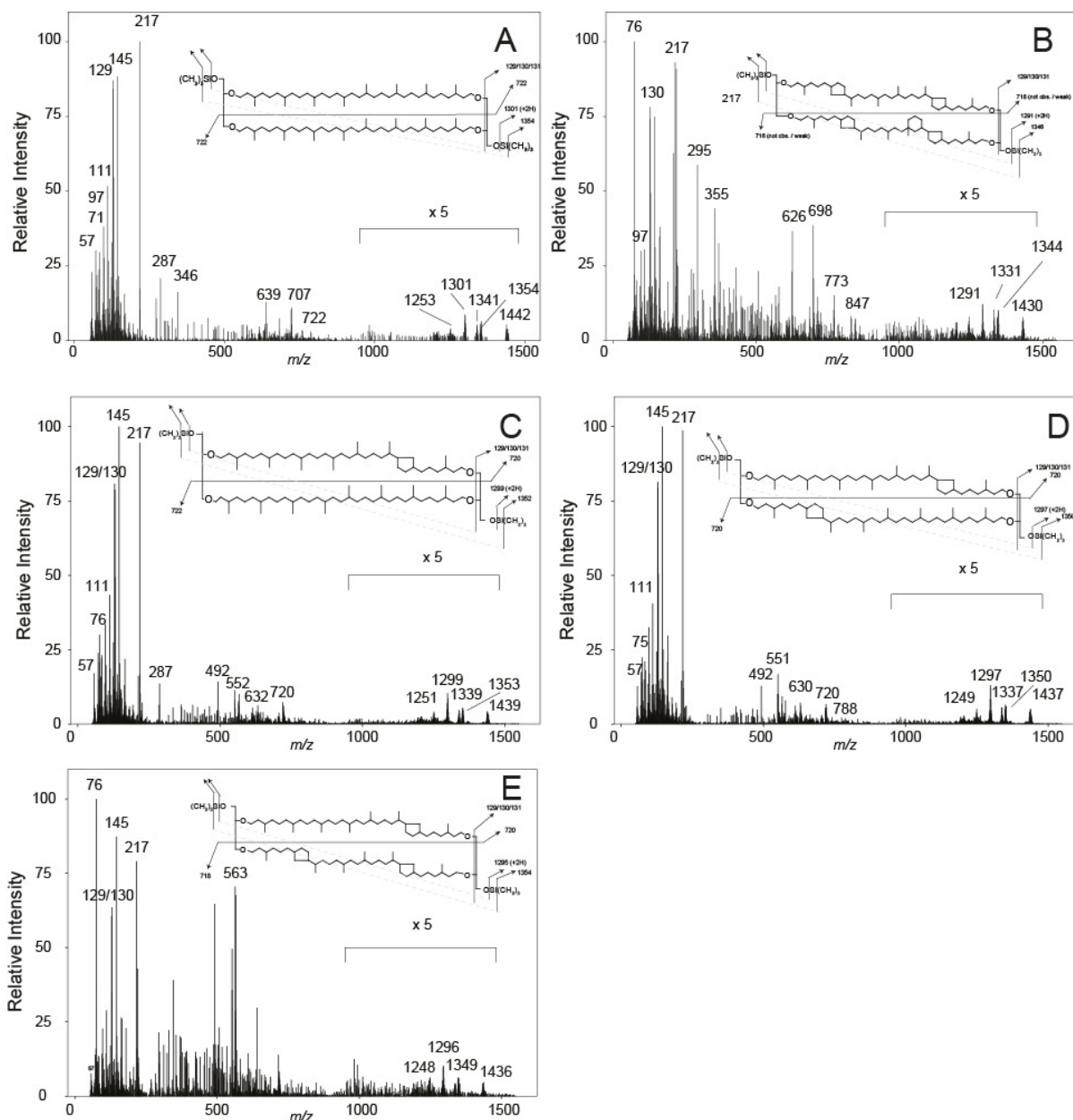


Figure S3. 70eV time-of-flight mass spectra of TMS-ethers of iGDGTs, obtained using HTGC-TOFMS: A) GDGT-0, B) crenarchaeol, C) GDGT-1, D) GDGT-2, and E) GDGT-3. Abundant  $m/z$  are shown and interpreted in the text. Fragmentation patterns are explained in Fig. S2.

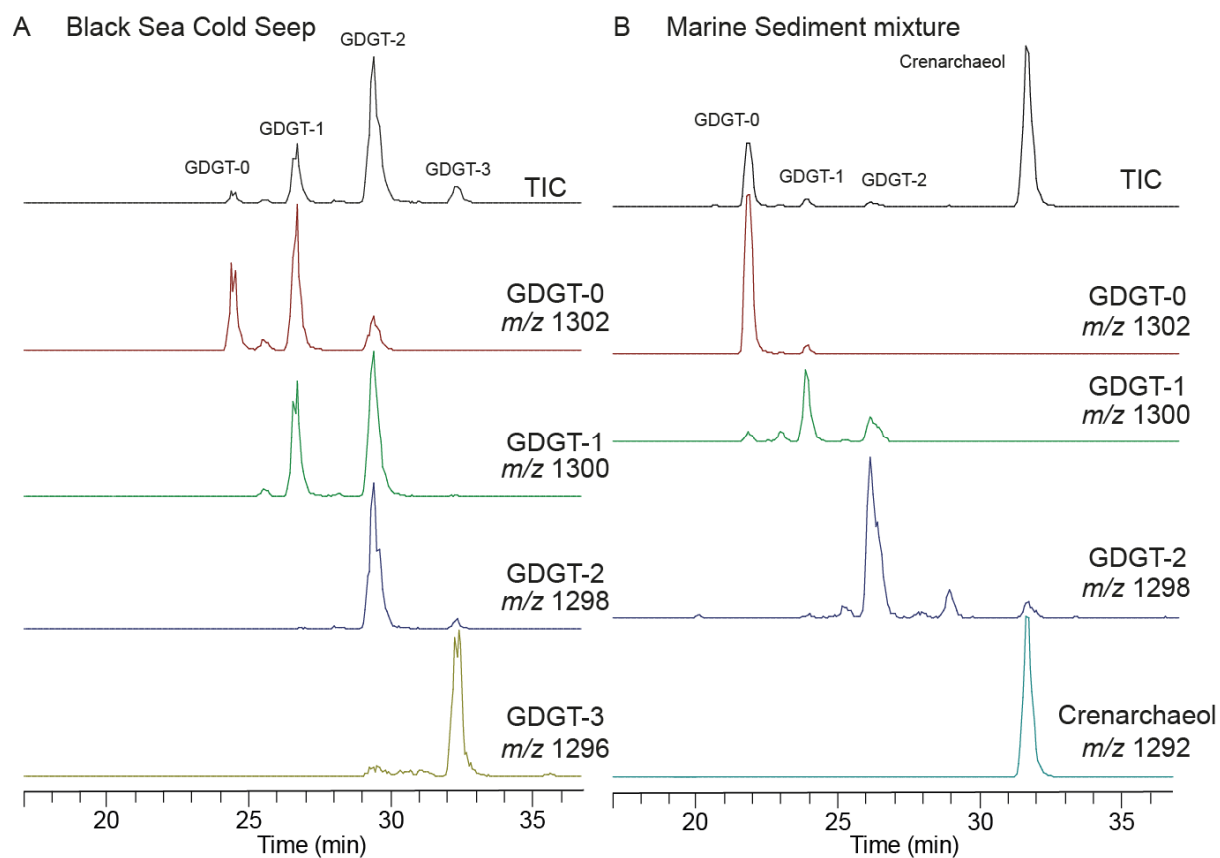


Figure S4. HPLC-APCI-MS chromatograms in selected ion monitoring (SIM) mode, showing iGDGTs (GDGT-0, -1, -2, -3 and Crenarchaeol) in samples used for comparison in this paper. The reconstructed total ion current and relevant SIM traces for iGDGTs (GDGT-0, -1, -2, -3 and Crenarchaeol) are shown: A) Black Sea cold seep sample; and B) extract of a mixture of marine sediments.

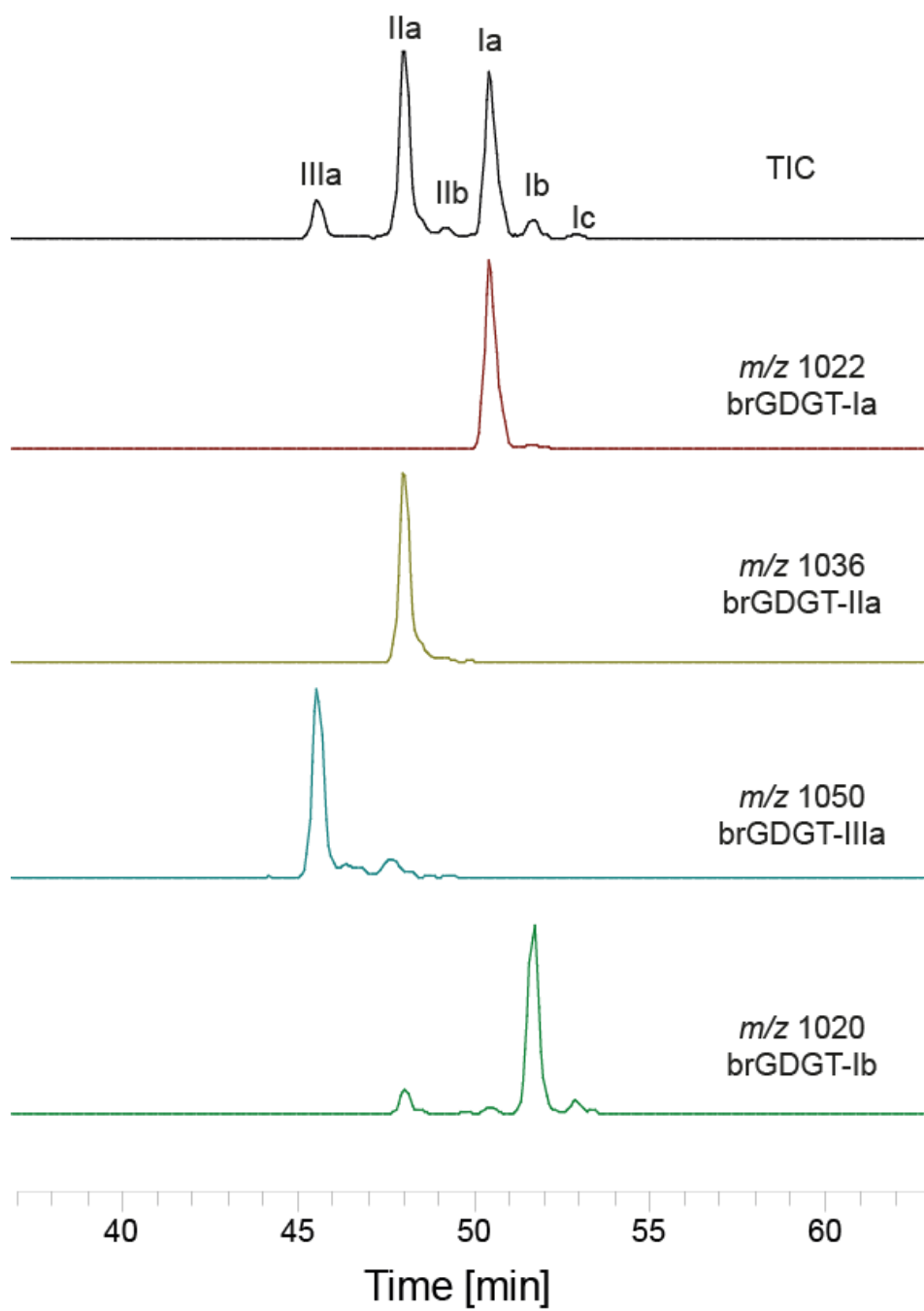


Figure S5. HPLC-APCI-MS chromatograms in SIM mode, showing brGDGTs. The reconstructed total ion current and relevant SIM traces for brGDGTs (Ia, IIa, IIIa, Ib, IIb) are shown.

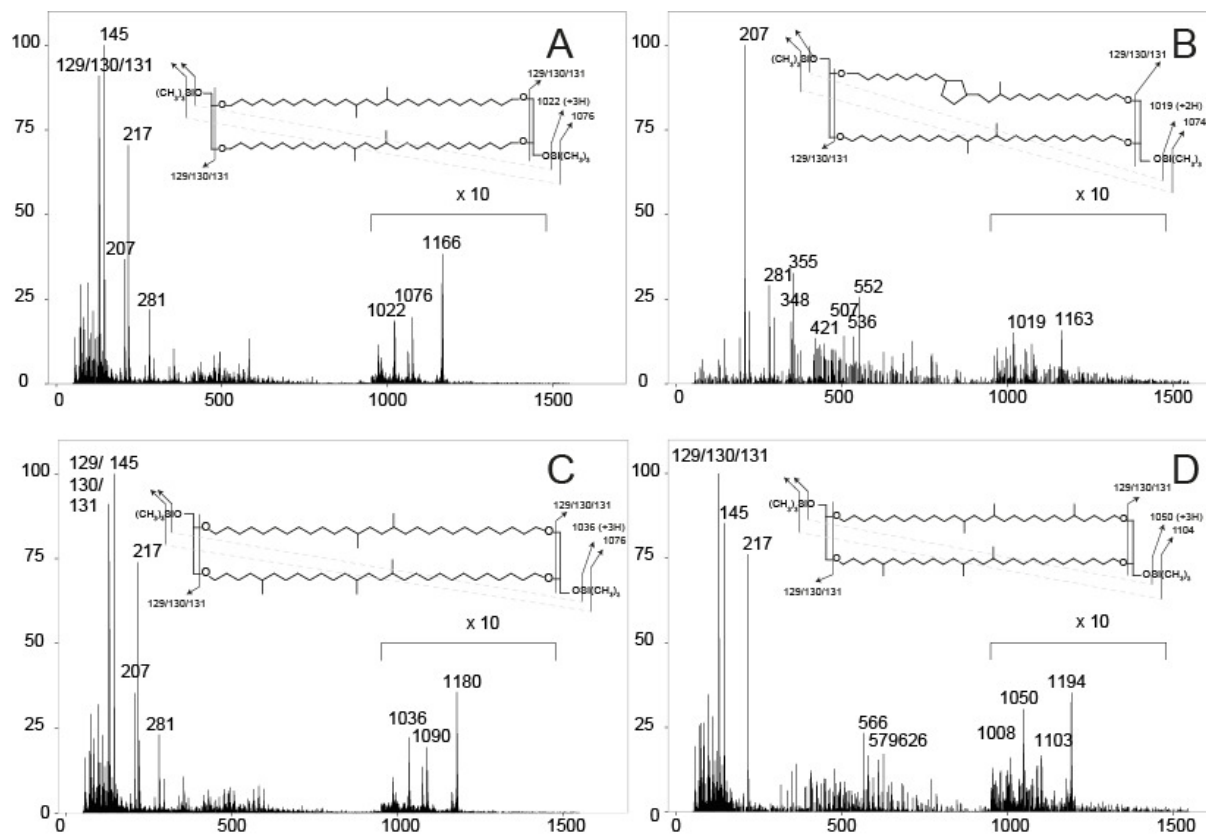


Figure S6. Mass spectra of TMS-ethers of brGDGTs, obtained using HTGC-TOFMS: A) GDGT-Ia, B) GDGT-Ib, C) GDGT-IIa, D) GDGT-IIIa.



Supplementary Table 1. Quantification of GDGT-0 based on trimyristin as an internal standard. Even though quantification was conducted using internal standard as common in GC, a linear regression of peak height vs. mass injected without correction, of the values in grey, was also calculated: Peak height [mV] = m(GDGT-0<sub>injected</sub>) [μg] . 2035 – 8.159, R<sup>2</sup> = 0.999, p = 5 . 10<sup>-7</sup>. \* Outlier

Mass injected [ug]		Peak height [mV]	Area [a.u.]		Area GDGT / Area TAG 1 <sub>norm</sub>
TAG 1	GDGT- 0	GDGT-0	TAG 1	GDGT- 0	
0.1077	0.14	279.8	8648	11992	0.1494
0.1077	0.07	128.4	9324	5505	0.0636
0.05385	0.035	133*	8440	5862	0.0374
0.02154	0.014	16.8	1244	691	0.0120
0.01077	0.0028	1.723	650.8	35.79	0.0006
0.01077	0.0014	1.2	438.1	14.78	0.0004
0.02154	0.00056	0.003	1534	9.49	0.0001
0.02154	0.0056	4.455	1468	131.1	0.0019
0.02154	0.0056	6.29	1324	121.7	0.0020
0.02154	0.0056	5.349	1550	141.51	0.0020

Supplementary Table 2. Mixing ratios of peat and marine standard and the determined relative abundances of GDGTs.

HPLC-APCI-MS		% Abundance			
%Marine	%Peat	GDGT-0	Cren	Sum brGDGTs	BIT
80	20	32	34	34	0.50
60	40	26	24	50	0.67
50	50	21	20	59	0.75
40	60	18	13	69	0.84
20	80	15	8	77	0.90
90	10	36	44	20	0.31
92	8	40	43	18	0.30
94	6	38	47	15	0.25
96	4	37	50	12	0.20
98	2	39	52	10	0.16
99	1	39	54	8	0.13
100	0	36	60	4	0.07

GC-FID		% Abundance				
%Marine	%Peat	GDGT-0	Cren	Sum brGDGTs	BIT	Molar BIT
80	20	28	31	41	0.57	0.63
60	40	22	19	60	0.76	0.80
60	40	22	20	59	0.75	0.79
80	20	27	30	42	0.58	0.63
50	50	19	14	67	0.83	0.86
40	60	17	11	73	0.87	0.90
20	80	13	6	81	0.93	0.94
90	10	31	43	26	0.38	0.43
92	8	32	42	25	0.37	0.43
94	6	34	44	22	0.34	0.39
96	4	35	49	16	0.25	0.30
98	2	38	49	13	0.21	0.25
99	1	37	51	11	0.18	0.21
100	0	40	54	6	0.10	0.12

